Seatific, Vol. 4, Issue. 2, pp. 37–47, December 2024

Seatific Journal
https://seatific.yildiz.edu.tr
DOI: https://doi.org/10.14744/seatific.2024.0006

Research Article

Development of a numerical modeling of the flow in an overtopping device with coupled Savonius turbine

Vinicius HEITMANN AVILA, Rafael Adriano Alves Camargo GONÇALVES, Jaifer Corrêa MARTINS, Emanuel da Silva Diaz ESTRADA, Liércio André ISOLDI, Luiz Alberto Oliveira ROCHA, Elizaldo Domingues DOS SANTOS*

Department of Mechanical Engineering, Federal University of Rio Grande (FURG), Rio, Brasil

ARTICLE INFO

Article history
Received: October 28, 2024
Revised: November 22, 2024
Accepted: November 26, 2024

Key words:
Numerical simulation; overtopping device; savonius turbine; sea wave energy

ABSTRACT

The study of the wave energy conversion (WEC) technologies has been growing, with an emphasis on the overtopping device. Its operation is based on a ramp that directs the wave water into an elevated reservoir. The accumulated water flows through a low-head turbine, generating electricity. This study proposes to develop a complete computational model to simulate a wave channel containing an overtopping device with a Savonius-type turbine inserted in the device's outlet duct. This study deals with the computational modeling of a multiphase (air and water), turbulent, incompressible flow with constant thermo physical properties, generated by the movement of numerical ocean waves. A validation study was conducted to guarantee the reliability of the separated models: i) flow in overtopping device without turbine, ii) flow over a free Savonius turbine. After this step, the two models are coupled and results showed that the coupling was successful, allowing the observation of the flow behavior in the complete model. Despite that, the computational model still needs adjustments to the turbine rotation and outlet channel geometry.

Cite this article as: Heitmann Avila V, Gonçalves RAAC, Martins JC, Estrada ESD, Isoldi LA, Rocha LAO, Dos Santos ED. Development of a numerical modeling of the flow in an overtopping device with coupled Savonius turbine. Seatific 2024;4:2:37–47.

1. INTRODUCTION

The demand for energy is expected to grow by more than 1.0% a year until 2040, which will increase the greenhouse gas emissions and the cost of generating energy with fossil fuels. This scenario brings economic challenges, energy security risks and geopolitical conflicts. In response, the current researches have focused on the development of technologies and the economic impact of renewable sources such as wind, solar, geothermal and wave energy (Jenniches, 2018).

The conversion of ocean energy into electricity is a renewable source with great potential, but which is still little explored globally. In the field of the wave energy, there is no dominant technology. Various devices have been proposed and studied, including point absorbers, attenuators, overtopping, submerged plates and oscillating water columns (Seibt et al., 2019).

The efficiency and durability of the wave energy converters are essential to making them competitive and economically viable. Overtopping and oscillating water column devices stand out for their simplicity and ease of maintenance, offering advantages in this context (Temiz et al., 2021).

Martins et al. (2022) investigated an overtopping device with one and two branches incorporated into a real breakwater, applying the Constructal Design method to analyze the effects of the degrees of freedom on the mean

***Corresponding author.**
*E-mail address: elizaldosantos@furg.br

dimensionless overtopping flow. The study compared different geometric configurations of the device to identify the best hydrodynamic performance, using the Joint North Sea Wave Project (JONSWAP) spectrum and the Volume of Fluid (VOF) model. The equations of mass conservation, momentum and transport of the volume fraction were solved. The results indicated that the two-ramp configuration led to 6.48% more overtopping than the one-ramp configuration, following the theoretical recommendations of Constructal Design for complex configurations. The study was carried out on the São José do Norte breakwater, RS, Brazil.

Santos et al. (2022) developed a computational model to investigate turbulent flows in an oscillating water column (OWC) device, considering a Savonius turbine in the air duct. Incompressible, two-dimensional, unsteady and turbulent flows were analyzed in three configurations: (1) a free turbine in a long channel for verification/validation, (2) a closed domain mimicking an OWC device with constant velocity at the inlet, and (3) the same domain with sinusoidal velocity at the inlet. A dynamic rotational mesh was used in the turbine region. The model, solving the unsteady time-averaged equations of conservation of mass and momentum with the *k-ω* SST (Shear Stress Transport) model, predicted power coefficients (C_p) similar to those in the literature for different tip speed ratios (0.75 ≤TSR ≤2.00). The closed domain increased the C_p compared to the free turbine, and the sinusoidal speed performed as well as the case of constant velocity imposed at the inlet of the domain.

Barros et al. (2023) carried out a numerical study of a full-scale overtopping device coupled to a seabed structure using the Constructal Design for geometric assessment. The aim was to investigate how the design influences the available power of the device, and the influence of the seabed structure in the device performance. The study considered the areas of the overtopping ramp (A_r) and the trapezoidal structure on the seabed (A_t) as constraints, exploiting two degrees of freedom: the ratio between the height and length of the ramp (H_3/L_3), and the ratio between the upper and lower bases of the trapezoidal obstacle (L_1/L_2), while the submergence is kept constant (H_1=3.5 m). The continuity, momentum and volume fraction transport equations were solved using the Finite Volume Method (FVM), and the water-air mixture was treated using the Volume of Fluid (VOF) model. The results indicated that H_3/L_3 had a greater impact on the water accumulated in the reservoir, but the inclusion of the coupled seabed structure increased the performance of the converter by 30% compared to a device without a structure.

Santos et al. (2023) developed a computational model to simulate an Oscillating Water Column (OWC) device coupled with a Savonius turbine. The device was inserted into a wave channel, with a Savonius turbine placed in the converter's inlet/outlet duct. The modeling used a moving rotational mesh, simulating the movement of the turbine under stabilized operating conditions, addressing the two-phase flow of air and water in the channel and the flow of air through the turbine. The model was verified for turbulent flow over a Savonius turbine and for wave flow in the converter without a turbine. The results showed that the model made it possible to calculate both the available power and the mechanical power of the turbine. In addition, for the studied conditions, the turbine did not cause significant changes in the behavior of the wave flow into the OWC chamber in comparison with the case without turbine. Despite that, an increase in the available power is noticed due to the restriction imposed by the turbine in the device. It is also noticed that the power coefficient also increased for similar range of TSR in comparison with the free turbine configuration.

Although there are several studies in the literature on overtopping devices, none have numerically evaluated the insertion of a turbine in these devices. This article seeks to fill this gap by analyzing a full-scale onshore overtopping device with a turbine inserted, an unprecedented investigation in the literature.

2. MATHEMATICAL AND NUMERICAL MODELING

2.1. Governing equations of the turbulent flows

For all simulations, the modeling of the incompressible, two-dimensional, unsteady and turbulent flows for a mixture of air and water is given by the unsteady time-averaged equations (URANS – Unsteady Reynolds-Averaged Navier Stokes) of mass conservation, momentum in the x and y directions, which are given by (Wilcox, 2006):

$$\frac{\partial \rho}{\partial t} + u\frac{\partial \rho}{\partial x} + v\frac{\partial \rho}{\partial y} + \rho\left(\frac{\partial \bar{u}}{\partial x} + \frac{\partial \bar{v}}{\partial y}\right) = 0 \quad (1)$$

$$\rho\left[\frac{\partial \bar{u}}{\partial t} + \bar{u}\frac{\partial \bar{u}}{\partial x} + \bar{v}\frac{\partial \bar{u}}{\partial y}\right] = -\frac{\partial \bar{p}}{\partial x} + (\mu + \mu_t)\left(\frac{\partial^2 \bar{u}}{\partial x^2} + \frac{\partial^2 \bar{u}}{\partial y^2}\right) \quad (2)$$

$$\rho\left[\frac{\partial \bar{v}}{\partial t} + \bar{u}\frac{\partial \bar{v}}{\partial x} + \bar{v}\frac{\partial \bar{v}}{\partial y}\right] = -\frac{\partial \bar{p}}{\partial y} + (\mu + \mu_t)\left(\frac{\partial^2 \bar{v}}{\partial x^2} + \frac{\partial^2 \bar{v}}{\partial y^2}\right) \quad (3)$$

where ρ is the fluid density (kg/m³), t is time (s), x and y are the spatial coordinates (m), u and v are the velocity components in the x and y directions, respectively (m/s), p is the pressure (N/m²), μ is the dynamic viscosity (kg/(m·s)), μ_t is the turbulent viscosity (kg/(m·s)), and the $\bar{u}$ and $\bar{v}$ represents the time-averaged velocities in x and y directions, respectively.

In the simulations of this study, two different phases are considered: air and water. Therefore, the concept of volume fraction (α_q) is used to represent the two phases within a control volume. In this model, the sum of the volume fractions within a control volume must be unitary ($0 \leq \alpha_q \leq 1$). Consequently, if α_{water}=0, the control volume is empty of water and full of air (α_{air}=1). If the fluid has a mixture of air and water, one phase is the complement of the other, i.e. $\alpha_{air} = 1 - \alpha_{water}$. Thus, an additional transport equation for one of the volume fractions is required (Hirt and Nichols, 1981):

$$\frac{\partial \alpha_{water}}{\partial t} + u\frac{\partial \alpha_{water}}{\partial x} + v\frac{\partial \alpha_{water}}{\partial y} + \alpha_{water}\left(\frac{\partial \bar{u}}{\partial x} + \frac{\partial \bar{v}}{\partial y}\right) = 0 \quad (4)$$

As the equations of conservation of mass and momentum are solved for the mixture, it is necessary to obtain the values of the density and viscosity for the mixture, which can be expressed as:

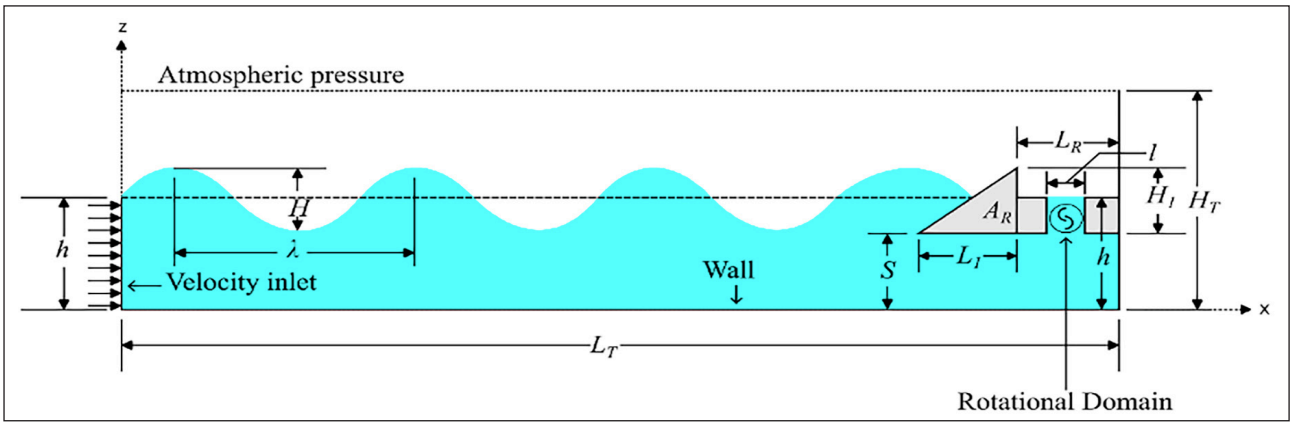

Figure 1. Computational domain of a full-scale overtopping device with an inserted turbine.

$$\rho = \alpha_{água}\rho_{água} + \left(1 - \alpha_{água}\right)\rho_{ar} \quad (5)$$

$$\mu = \alpha_{água}\mu_{água} + \left(1 - \alpha_{água}\right)\mu_{ar} \quad (6)$$

For the *k*-*ω* SST closure model, the turbulent viscosity (μ_t) is given by (Menter, Kuntz and Langtry, 2003):

$$\mu_t = \frac{\bar{\rho}\alpha_1 k}{max(\alpha_1\omega, SF_2)} \quad (7)$$

The transport equations for turbulent kinetic energy (k) and its specific dissipation rate (ω) are computed as (Menter, Kuntz and Langtry, 2003):

$$\frac{\partial k}{\partial t} + \frac{\partial(\overline{u_i}k)}{\partial x_i} = \tilde{P}_k - \frac{k^{\frac{2}{3}}}{L_T} + \frac{\partial}{\partial x_i}\left[(\mu + \sigma_k\mu_t)\frac{\partial k}{\partial x_i}\right] \quad (8)$$

$$\frac{\partial \omega}{\partial t} + \frac{\partial(\overline{u_i}\omega)}{\partial x_i} = \frac{\alpha}{\mu_t}\tilde{P}_k - \beta\omega^2 + \frac{\partial}{\partial x_i}\left[(\mu + \sigma_\omega\mu_t)\frac{\partial \omega}{\partial x_i}\right] + 2(1 - F_1)\frac{\sigma_{\omega 2}}{\omega}\frac{\partial k}{\partial x_i}\frac{\partial \omega}{\partial x_i} \quad (9)$$

in which $\tilde{P}_k$ is a function that prevents the generation of turbulence in regions of stagnation, i represents the direction of the fluid flow (i=1 represents the x direction and i=2 represents the y direction), β=0.09, α_1=5/9, β_1=3/40, σ_k=0.85, σ_ω=0.5, σ_2=0.44, β_2=0.0828, σ_{k2}=1 and $\sigma_{\omega 2}$=0.856 are constants used in Menter (1993). The mixing functions F_1 and F_2 are defined by the following equations (Menter, Kuntz and Langtry, 2003):

$$F_1 = \tanh\left\{\left\{min\left[max\left(\frac{k^{\frac{1}{2}}}{\beta^*\omega y}, \frac{500v}{y^2\omega}\right), \frac{4\rho\sigma_{\omega 2}k}{CD_{k\omega}y^2}\right]\right\}^4\right\} \quad (10)$$

$$F_2 = \tanh\left\{\left[max\left(\frac{2k^{\frac{1}{2}}}{\beta^*\omega y}, \frac{500v}{y^2\omega}\right)\right]^2\right\} \quad (11)$$

In equation (10), the term $CD_{k\omega}$ is given by (Menter, Kuntz and Langtry, 2003):

$$CD_{k\omega} = max\left(2\rho\sigma_{\omega 2}\frac{1}{\omega}\frac{\partial k}{\partial x_i}\frac{\partial \omega}{\partial x_i}, 10^{-10}\right) \quad (12)$$

2.2. Description of the case study

The physical problem analyzed here consisted of a two-dimensional overtopping device placed in a wave channel with a Savonius turbine inserted, as shown in Figure 1. The third-dimension y is perpendicular to the plane of the figure. The wave motion was generated by imposing a velocity field on the left surface of the tank. In this study, the ratio between the areas of the ramp and the wave channel were kept fixed (ϕ=A_r/A_T=0,012). Other parameters adopted in this study were: H_T/L_T=0,0612 (ratio between tank height, H_T=20 m, and tank length, L_T=327 m) and H/h=0.1 (ratio between wave height, H=1 m, and water depth, h=10 m). In addition, a reservoir with length of L_R=20 m and a height range for the device of S=6 m were also considered. For this value of S, the ratio H_l/L_l = 0.14 was simulated.

In the region of the turbine, a constant angular velocity (η) of 0.5 rad/s was imposed in the region called the rotational domain (Fig. 1), simulating the effect of the fluid action on the turbine. A non-slip and impermeable boundary condition was imposed on the walls of the turbine ($u = v =$ 0 m/s) related to the rotational domain. The duct where the turbine is located has a width (l) equal to 2.344 m.

Regarding the other boundary conditions, an atmospheric pressure of P_{abs} = 101.3 kPa was applied to the upper region of the left lateral surface and the upper surface (dashed surfaces in Fig. 1). A no-slip and impermeability conditions ($u = w =$ 0 m/s) were imposed on the lower and right-side surfaces and on the surface of the overtopping device.

The initial conditions are that the fluid is wavy and that the water surface has a free surface with a height of h=10 m. As far as wave generation is concerned, a velocity profile was imposed at the channel entrance (left lateral surface of Fig. 1), simulating the operation of a wave generator (Horko, 2007). The velocity components in the wave propagation (x) and vertical (z) directions for the entrance channel are based on the second-order Stokes theory and are expressed, respectively, by (Chakrabarti, 2005):

$$u = \frac{gH}{2c}\frac{\cosh[k(z+h)]}{\cosh(kh)}\cos(kx - \omega t) + \frac{3}{16}ck^2H^2\frac{\cosh[2k(z+h)]}{\sinh^4(kh)}\cos[2(kx - \omega t)] \quad (13)$$

$$w = \frac{gH}{2c}\frac{\sinh[k(z+h)]}{\cosh(kh)}\sin(kx - \omega t) + \frac{3}{16}ck^2H^2\frac{\sinh[2k(z+h)]}{\sinh^4(kh)}\sin[2(kx - \omega t)] \quad (14)$$

$$\eta = \frac{H}{2}\cos(kx - \omega t) + \frac{kH^2}{16}\frac{\cosh(kh)}{\sinh^3(kh)}[2 + \cosh(2kh)]\cos[2(kx - \omega t)] \quad (15)$$

Table 1. Characteristics of regular waves

Parameter	Symbol	Magnitude
Wave height	H	1.00 m
Wave period	T	7.50 s
Wave length	λ	65.4 m
Channel depth	h	10.00 m

where H is the wave height (m), k is the wave-number given by $k=2\pi/\lambda$ (m^{-1}), h is the water depth (m), T is the wave period (s), $\lambda=2\pi/T$ is the frequency (rad/s), t is the time (s), c is the wave celerity (m/s) and ω is the angular velocity (Hz). Table 1 shows the characteristics adopted for the waves considered in this study.

3. NUMERICAL PROCEDURES

This work used the Finite Volume Method (FVM) (Versteeg and Malalasekera, 2007) for the numerical solution of the equations of conservation of mass, momentum and the volume fraction transport equation. The commercial Computational Fluid Dynamics (CFD) package FLUENT™ was also used. The multiphase Volume of Fluid (VOF) model (Hirt and Nichols, 1981) was applied to the interaction between air, water and the device. The numerical parameters adopted in the ANSYS FLUENT 2022 commercial software are shown in Table 2.

As for the spatial discretization, a stretch mesh was considered, following the recommendations of Gomes et al. (2012) for the wave channel, Martins et al. (2022) for the overtopping device, and Santos et al. (2022) in the Savonius turbine. However, greater refinement was adopted both in the free surface region, where 30 volumes per wave height were used, and horizontally, where 70 volumes per wavelength were considered, as defined by the mesh independence test. The interaction between the wave flow and the ramp of the overtopping device justifies this greater refinement, resulting in approximately 155,000 finite volumes. Figure 2 illustrates the mesh generated by the GMSH software for the computational domain, detailing the region of the overtopping device and the turbine.

Regarding the spatial discretization of the Savonius turbine, triangular and rectangular hybrid finite volumes were used in the computational domain (Santos et al., 2022). Figure 3 illustrates the turbine mesh, Figure 3a, and a detail of the mesh on the blades, Figure 3b, respectively. In detail, it is possible to see a region around the blades with a refined rectangular mesh.

4. RESULTS AND DISCUSSION

Firstly, the validation of the present numerical method for solving of the isolated cases of overtopping (without turbine and exit duct connected to the reservoir) and free Savonius turbine subjected to turbulent air flow is performed.

For the overtopping device, the numerical model used, based on Goulart et al. (2015), was verified, as shown in Figure 4. To do this, a comparison was made between the height of the water accumulated in the reservoir as a function of time obtained in the author's numerical study and the numerical predictions obtained with the current computational method. This comparison is presented in Figure 5.

As can be seen, the numerical results were in close agreement. The numerical results also predicted the onset of overtopping (t~47 s) and the slope of the water accumulation curve in the reservoir. It is therefore possible to state that this computational method is verified.

Table 2. Methods used in numerical simulations

Parameter	Numerical input
Solver	Pressure-based
Pressure-velocity coupling	PISO
Spatial discretization	
Gradient evaluation	Least squares cell based
Pressure	PRESTO
Momentum	First order upwind
Volume fraction	Geo-reconstruct
Temporal differencing scheme	First order implicit
Regime flow	k-ω SST
Under-relaxation factors	
Pressure	0.3
Momentum	0.7
Residual	
Continuity	10^{-6}
Velocity-x	
Velocity-z	
Open channel initialization method	Wavy
Time step (Δt)	2.00×10^{-2} s
Maximum number of iterations per time step	200

PISO: Pressure implicit with split operator; PRESTO: Pressure staggering option; SST: Shear Stress Transport

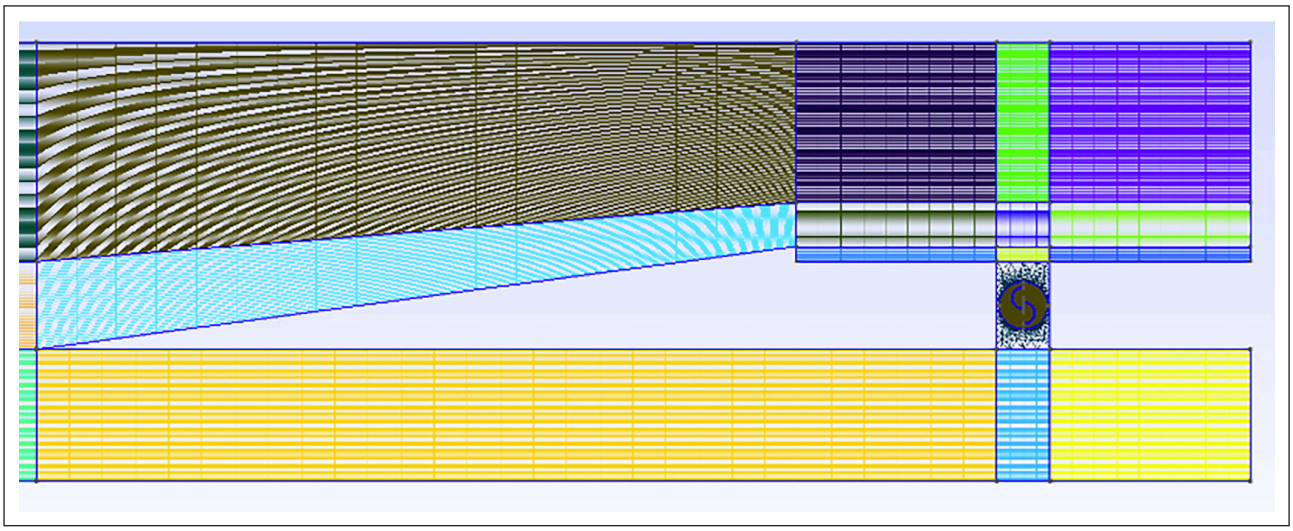

Figure 2. Spatial discretization applied to the full-scale overtopping device with an inserted turbine.

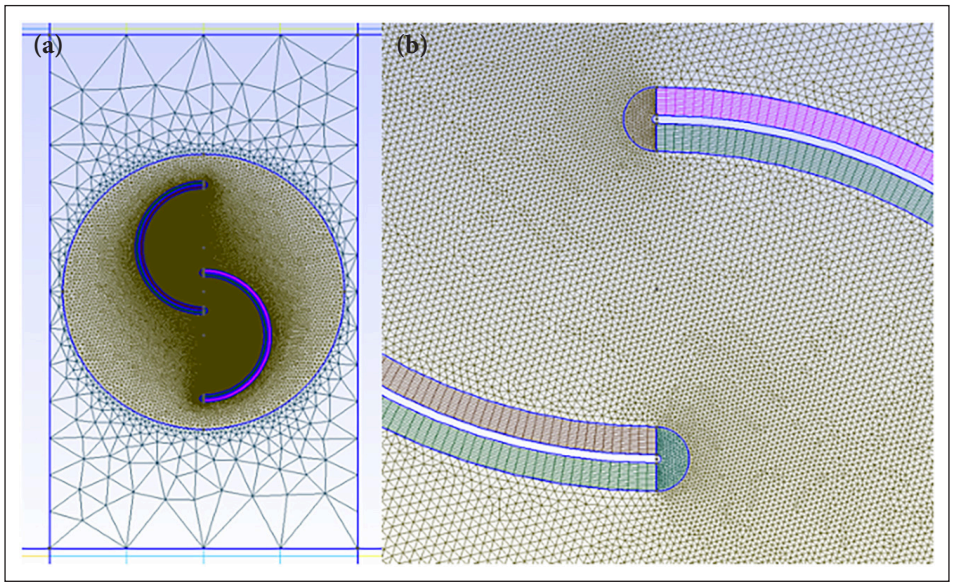

Figure 3. Mesh used in the Savonius turbine region: (a) overview of the entire turbine, (b) mesh refinement detail of the blade surfaces.

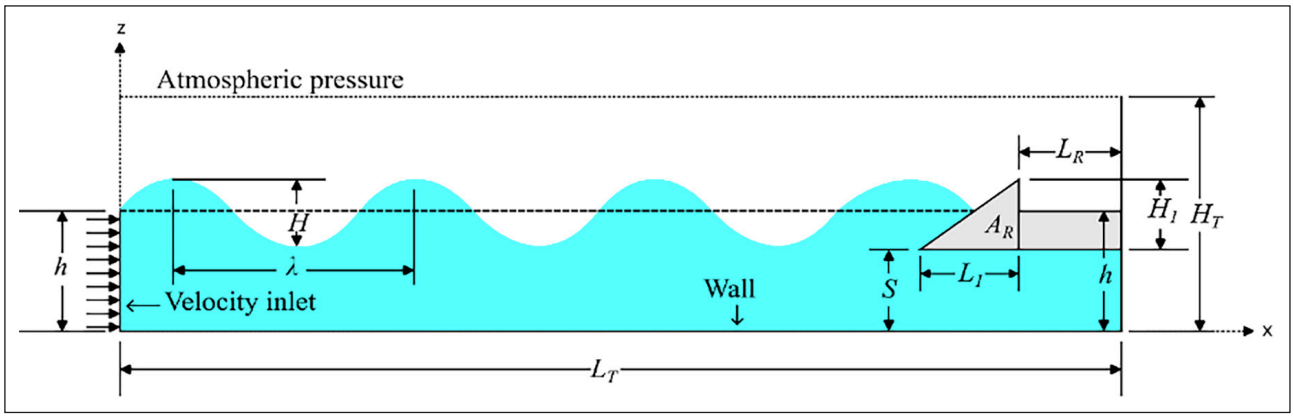

Figure 4. Schematic representation of the domain investigated numerically by Goulart et al. (2015).

For the Savonius turbine, validation of the numerical model was carried out by comparing the results obtained for the power coefficient with the experimental work of Blackwell et al. (1977) and with the numerical works of Akwa et al. (2012) and Santos et al. (2022) for the different tip speed ratios (TSR): 0.75; 1.00; 1.25 and 2.00. Free-flowing air flows with a constant

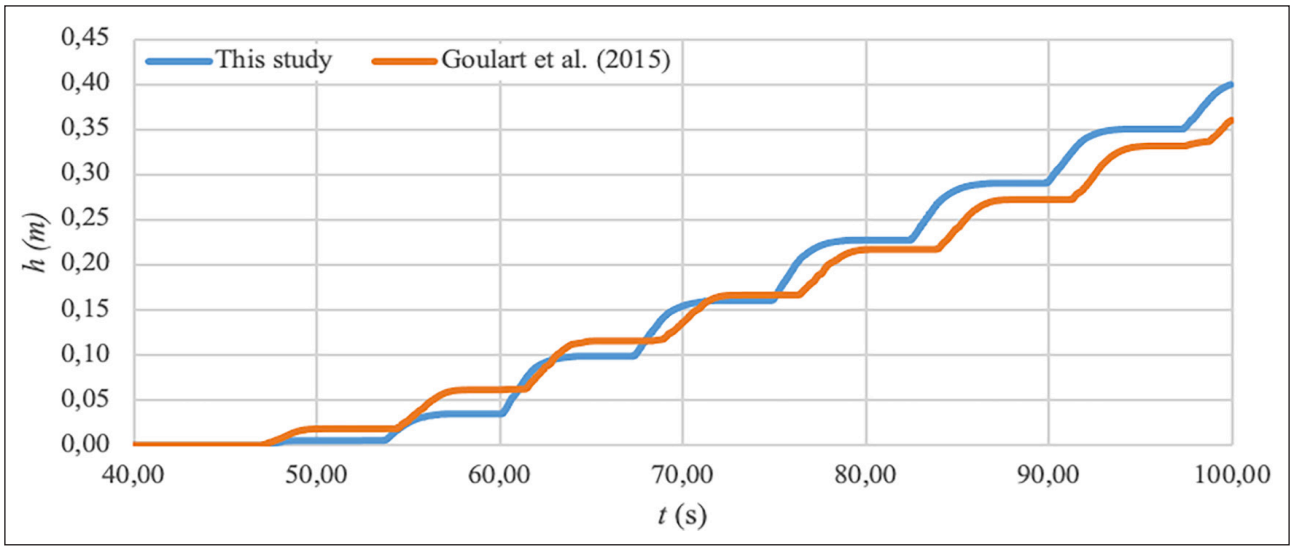

Figure 5. Water accumulated in the reservoir of the overtopping device as a function of time obtained numerically in Goulart et al. (2015) and with the present method.

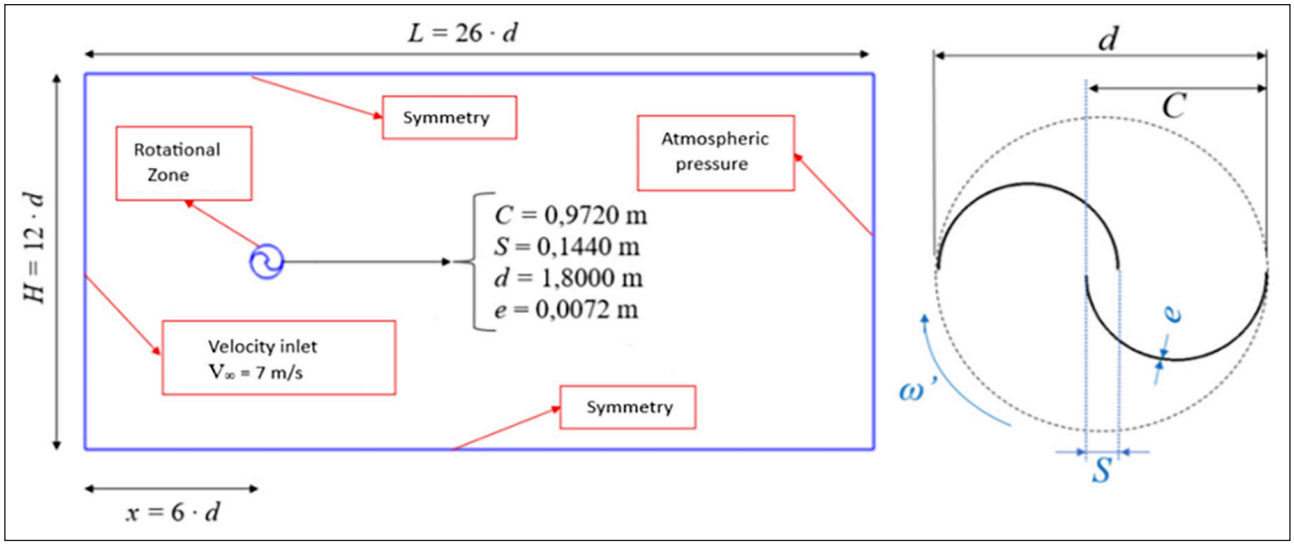

Figure 6. Computational domain of the wind tunnel with a Savonius turbine.

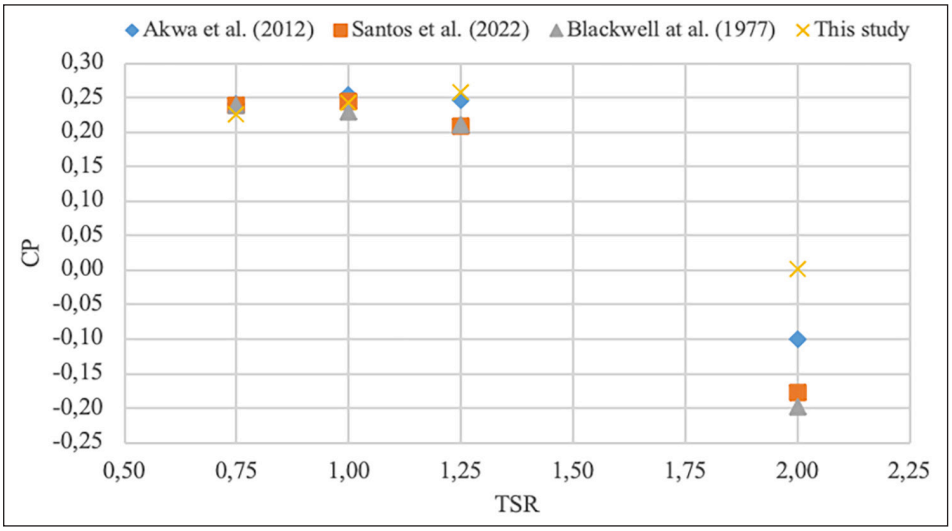

Figure 7. Numerical validation of C_p for Savonius turbine in a wind tunnel.

TSR: Tip speed ratios.

Table 3. Power coefficient for different tip speed ratios

TSR	C_p			
	Akwa et al. (2012)	**Santos et al. (2022)**	**Blackwell et al. (1977)**	**This study**
0.75	0.240	0.238	0.238	0.225
1.00	0.255	0.244	0.230	0.243
1.25	0.247	0.210	0.210	0.257
2.00	-0.100	-0.177	-0.199	0.002

TSR: Tip speed ratios

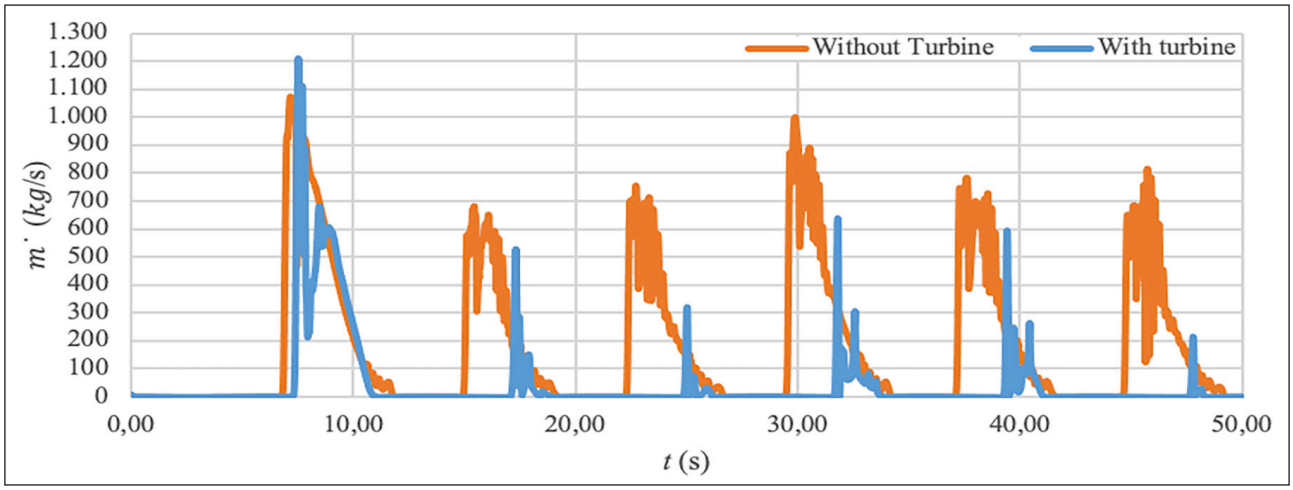

Figure 8. Instantaneous behavior of the water in the overtopping device for the cases without turbine and with turbine inserted over the mass flow.

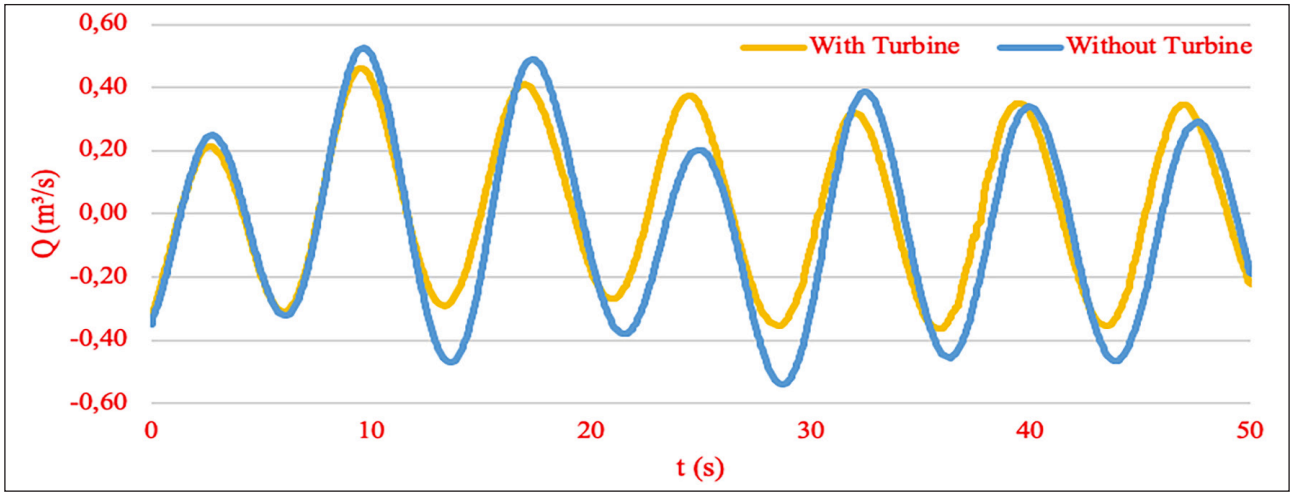

Figure 9. Instantaneous behavior of the water flow over the exit duct in the overtopping device.

velocity of $V_\infty = 7$ m/s and a Reynolds number of $R_{eD} = 867{,}000$ in the rectangular domain impinging a rotational turbine is investigated. The domain analyzed with its dimensions and boundary conditions is shown in Figure 6. The computational mesh for validation was generated in such a way as to be as close as possible to the work of Santos et al. (2022).

The pressure-based solver was used for the simulations of this numerical validation using the ANSYS FLUENT 2022 R2 program. The spatial discretization for the pressure was treated with the second-order formulation, while the second-order upwind is adopted for the equations of the momentum. For the pressure-velocity coupling, the SIMPLE algorithm was employed. For the closure of the turbulence, the k-ω SST turbulence model was implemented.

Figure 7 illustrates and Table 3 presents the comparison of the results of the effect of the blade tip speed ratio on the power coefficient (C_p) of the present work with the experimental and numerical works.

With the results obtained, the numerical validation of the rotating Savonius turbine in a two-dimensional domain simulating a wind tunnel, according to the experimental study by Blackwell et al. (1977) and the numerical study by Akwa et

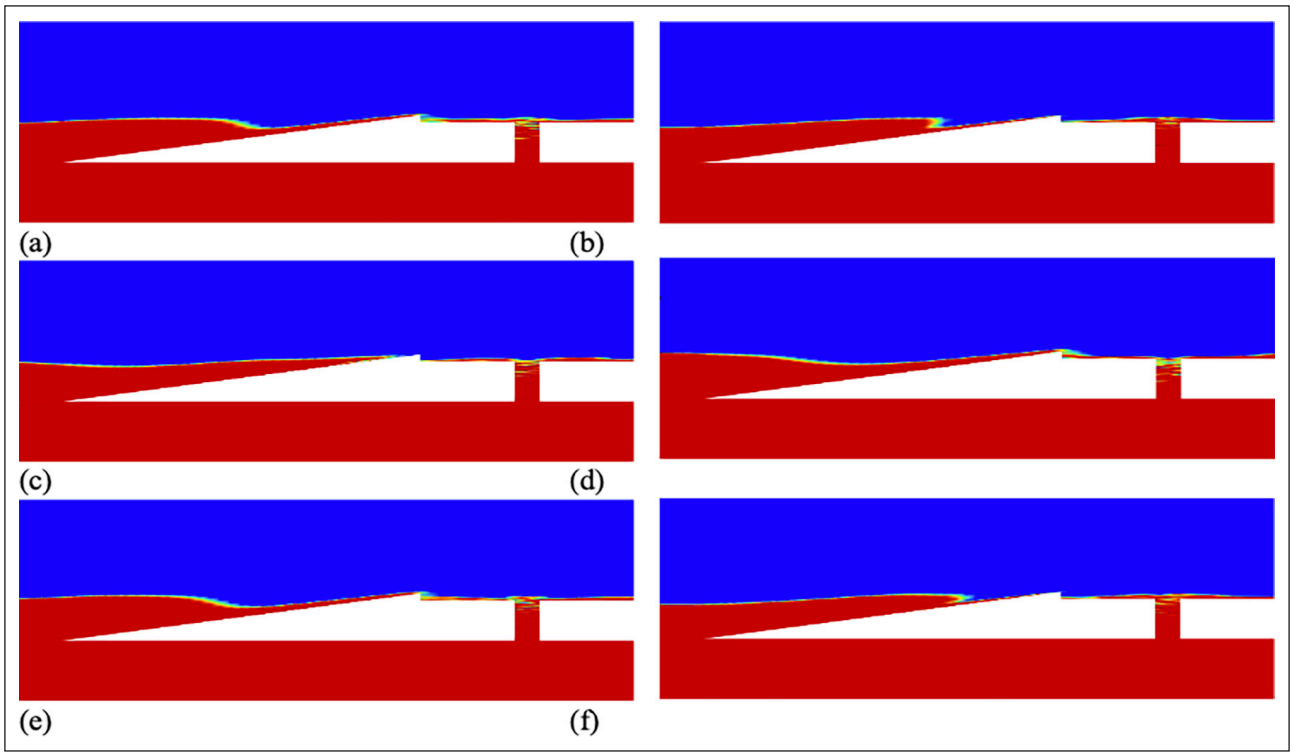

Figure 10. Wave flow as function of time for the cases without turbine: (a) t = 40.0 s, (b) t = 42.0 s, (c) t = 44.0 s, (d) t = 46.0 s, (e) t = 48.0 s and (f) t = 50.0 s.

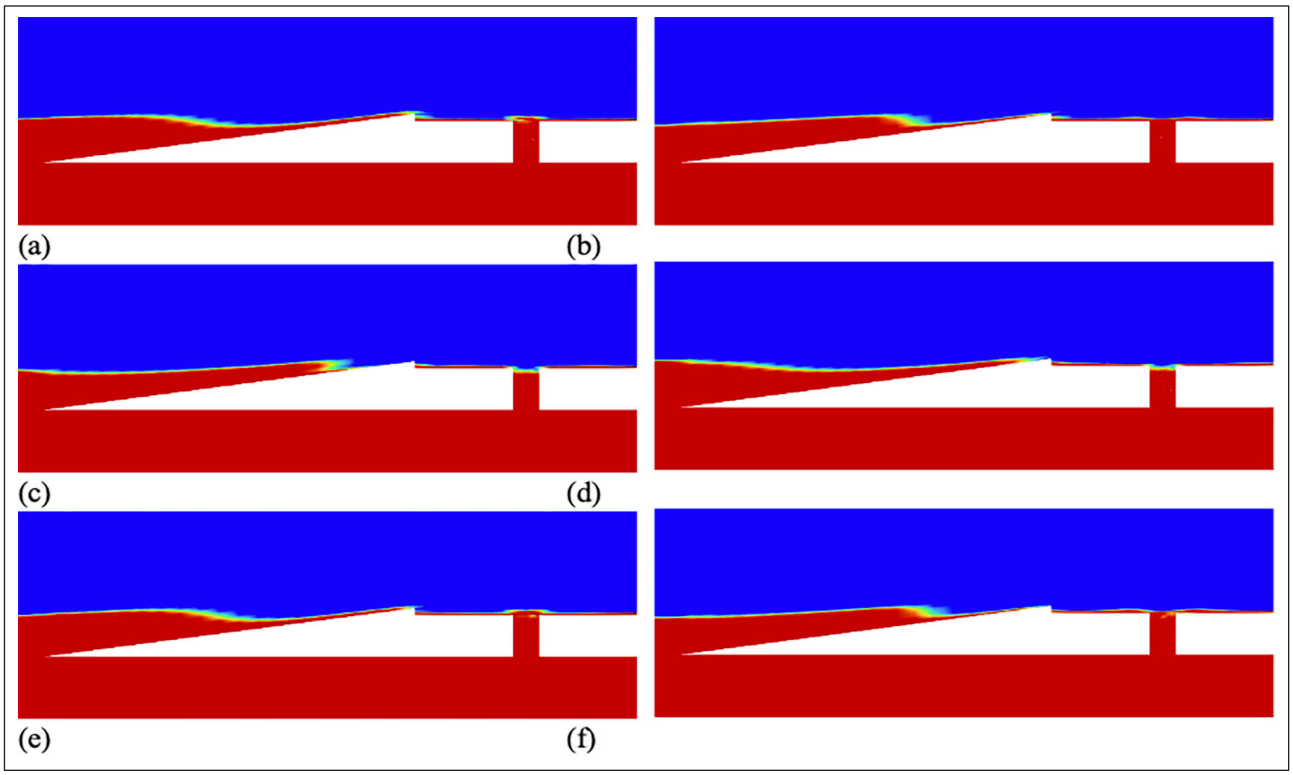

Figure 11. Wave flow as function of time for the cases with turbine: (a) t = 40.0 s, (b) t = 42.0 s, (c) t = 44.0 s, (d) t = 46.0 s, (e) t = 48.0 s and (f) t = 50.0 s.

al. (2012), was considered satisfactory for the continuation of the coupled model proposed in the present study.

Based on the results obtained in the validation studies for each case (overtopping without turbine, and free flow over a Savonius turbine) it is presented here onward the analysis of the overtopping device with the coupled Savonius turbine and some comparison with the overtopping device with the exit duct, but without the turbine mounted in the device.

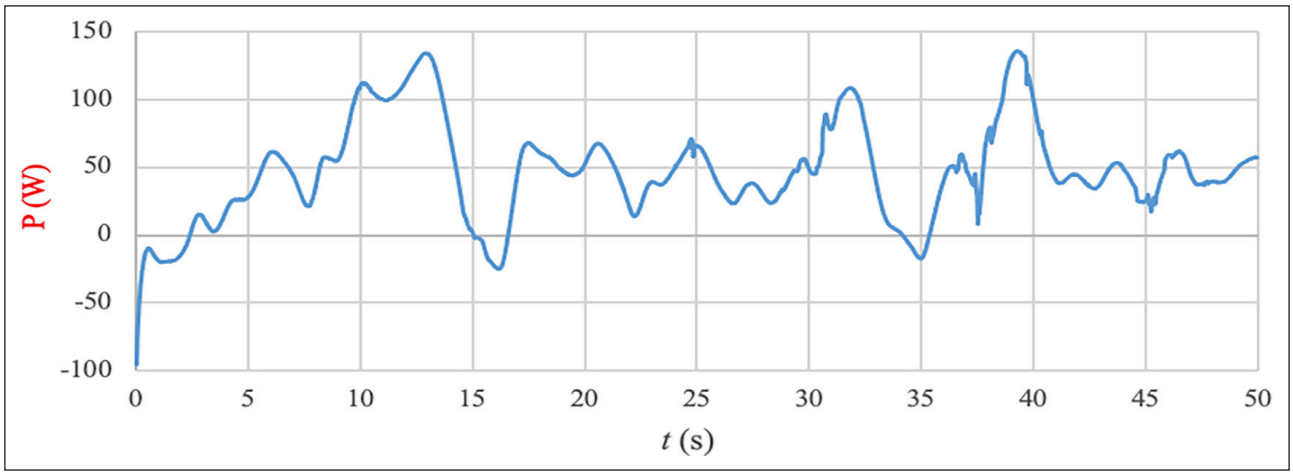

Figure 12. Power extracted from the turbine as a function of time.

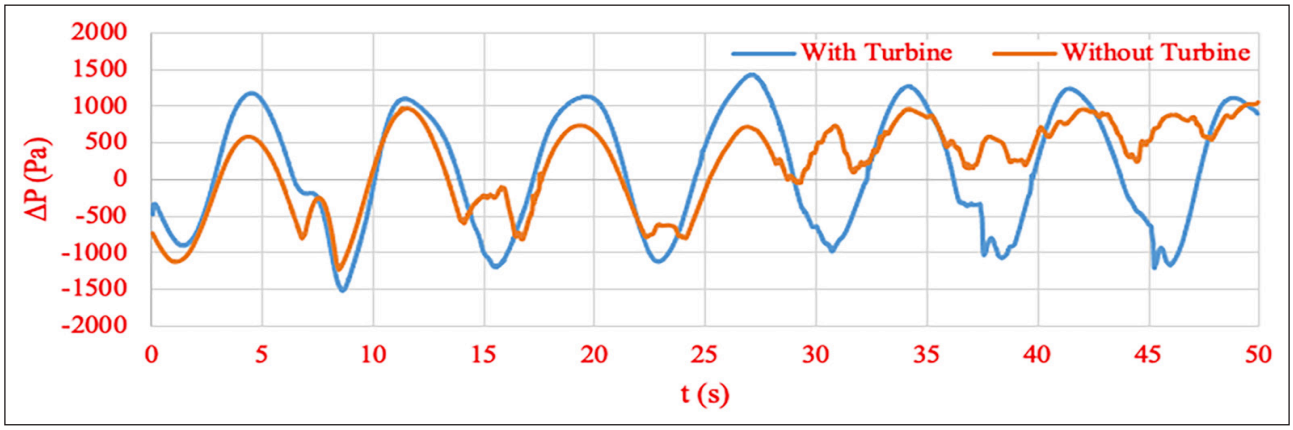

Figure 13. Turbine pressure gradient as a function of time.

Figure 8 shows the instantaneous behavior of the water in the overtopping device on the mass flow rate ($\dot{m}$), for the cases with turbine (Fig. 1) and the same case, but without the turbine insertion. The measure of mass flow rate is recorded by means of a probe placed at the top of the ramp of the device until the end of the reservoir. The results demonstrated that the insertion of the turbine affected the arriving of the wave flow oncoming the ramp, changing the mass flow rate of water overtopping the device, mainly from the second overtopping peak onwards. Figure 8 also shows that, for the two cases analyzed, the mass flow peaks began to occur at a time approximately t~7 s. Both for the situation of the overtopping device without the turbine and with the turbine, the highest magnitudes were observed at t~7 s, being $\dot{m}$=1074.80 kg/s and $\dot{m}$=1212.51 kg/s, respectively. It is important to note that the case of the overtopping device without the turbine inserted obtained a greater accumulation of mass flow compared to those with the turbine inserted, since part of the wave's energy ends up causing a return of the water flow through the duct where the device's turbine is located. Figure 9 shows the instantaneous behavior of the water flow over the exit duct in the overtopping device. In both cases, it can be noticed a pulsating behavior of the flow, which can affect the dynamic of the fluid flow in the frontal region of overtopping device. Figures 10 and 11 show the volume fraction of water in the time interval of 40.0 s ≤ t ≤ 50.0 s for the cases without and with turbine, respectively, considering different instants of time: (a) t = 40.0 s; (b) t = 42.0 s; (c) t = 44.0 s; (d) t = 46.0 s; (e) t = 48.0 s; and (f) t = 50.0 s. The results of the volume fraction illustrate the influence of the flow exiting the power take off region on the wave flow has in the wave flow overtopping the device.

Figures 12 show the power extracted from the turbine and Figure 13 show the pressure gradient in the exit duct for the cases without and with turbine. Based on this data, it was possible to determine the power coefficient C_p and the turbine tip speed, which are equal to 0.12 and 1.85, respectively. The positive magnitude of C_p obtained indicates that the fluid flow provides energy for the device. Despite that, the magnitude of CP for a Savonius turbine can achieve higher magnitudes, showing that the investigation of the imposed rotation and geometric configuration of the exit duct should be analyzed in more detail in future studies. Nevertheless, the developed model is promising for future investigations on the overtopping device in a more realistic approach.

5. CONCLUSION

This study carried out a two-dimensional analysis of an overtopping-type wave energy converter combined with a Savonius rotation turbine in the outlet duct. The simulations

used the Finite Volume Method (FVM) and the Volume of Fluid (VOF) methodology to model the interaction between air and water, with waves generated from the 2nd order Stokes theory. The turbine was included in the model, in a moving mesh with constant angular velocity. The κ-ω SST turbulent model was used to close the equations, and the geometry and meshes were generated in GMSH, while the processing was carried out in ANSYS FLUENT 2022 R2.

Firstly, the present computational model was validated for two isolated cases of overtopping device without turbine and exit duct in the reservoir, and free turbine under turbulent air flow. Later, a comparison of two cases (one with and other without turbine, but with the exit duct) was performed. The results showed that the greatest amount of water entering the reservoir over time was obtained for the case of the overtopping device without the turbine. The insertion of the turbine in the exit duct of the overtopping device conducted to a less amount of water passing through the turbine conduit, affecting the behavior of the wave oncoming the ramp. This difference is reflected in the instantaneous mass flow rate of water entering in the reservoir, mainly from the second occurrence onward.

In general, the developed computational modeling was promising in reproduce the behavior of the device with a coupled turbine, which is a novelty here. However, future studies are required to investigate the rotation (in the present model) that conducts to the highest power coefficient and the design of the exit duct that improves the turbine performance.

ACKNOWLEDGMENTS

The author V. H. Avila thanks CNPq for the master's scholarship (Process: 132159/2023-6) and ANP for the post-doctoral scholarship (Process: 2024/12385-9). The authors L. A. Isoldi, L. A. O. Rocha and E. D. dos Santos thank CNPq for the research productivity grant (Processes: 309648/2021-1, 307791/2019-0, 308396/2021-9). The authors would like to thank CNPq for financial support under CNPq/MCTI Call No. 10/2023 - Universal (Process: 403408/2023-7). L.A.O. Rocha and E.D. dos Santos also thank Fundação para a Ciência e Tecnologia, I.P. (doi.org/10.54499/UIDP/04683/2020 ; doi.org/10.54499/UIDB/04683/2020).

DATA AVAILABILITY STATEMENT

The authors state that the published publication includes all graphics and data collected or developed during the study.

CONFLICT OF INTEREST

The author declared no potential conflicts of interest with respect to the research, authorship, and/or publication of this article.

ETHICS

There are no ethical issues with the publication of this manuscript.

USE OF AI FOR WRITING ASSISTANCE

No AI technologies utilized.

FINANCIAL DISCLOSURE

The work was funded by CNPq and CAPES.

REFERENCES

Akwa, J. V., Silva Júnior, G. A., & Petry, A. P. (2012). Discussion on the verification of the overlap ratio influence on performance coefficients of a Savonius wind rotor using computational fluid dynamics. *Renewable Energy, 38*(1), 141–149. [CrossRef]

ANSYS FLUENT. (2022). *Documentation Manual*. ANSYS FLUENT 2022 R1.

Barros, A. S. de, Fragassa, C., Paiva, M. da S., Rocha, L. A. O., Machado, B. N., Isoldi, L. A., Gomes, M. das N., & Santos, E. D. dos. (2023). Numerical study and geometrical investigation of an onshore overtopping device wave energy converter with a seabed coupled structure. *Journal of Marine Science and Engineering, 11*(2), Article 412. [CrossRef]

Blackwell, B. F., Sheldahl, R. E., & Feltz, L. V. (1977). *Wind tunnel performance data for two-and three-buckets savonius rotors (final report SAND76-0131)*. Sandia Laboratories.

Chakrabarti, S. K. (2005). *Handbook of offshore engineering*. Elsevier.

Gomes, M. N., Isoldi, L. A., Santos, E. D., & Rocha, L. A. O. (2012). *Análise de Malhas para Geração Numérica de Ondas em Tanques. In VII Congresso Nacional de Engenharia Mecânica* – CONEM, São Luís, Maranhão, Brasil.

Goulart, M. M., Martins, J. C., Acunha Júnior, I. C., Gomes, M. N., Souza, J. A., Rocha, L. A. O., Isoldi, L. A., & Santos, E. D. (2015). Constructal design of an onshore overtopping device in real scale for two different depths. *Marine Systems & Ocean Technology, 10,* 120–129. [CrossRef]

Hirt, C. W., & Nichols, B. D. (1981). Volume of fluid (VOF) method for the dynamics of free boundaries. *Journal of Computational Physics, 39*(1), 201–225. [CrossRef]

Horko, M. (2007). *CFD Optimisation of an oscillating water column energy converter* [Master's thesis]. School of Mechanical Engineering, The University of Western Australia.

Jenniches, S. (2018). Assessing the regional economic impacts of renewable energy sources – a literature review. *Renewable and Sustainable Energy Reviews, 93*, 35–51. [CrossRef]

Martins, J. C., Fragassa, C., Goulart, M. M., Santos, E. D. dos, Isoldi, L. A., Gomes, M. das N., & Rocha, L. A. O. (2022). Constructal design of an overtopping wave energy converter incorporated in a breakwater. *Journal of Marine Science and Engineering, 10*(4), Article 471. [CrossRef]

Menter, F. R. (1993). *Zonal two equation k–ω turbulence models for aerodynamic flows*. In Proceedings of the AIAA 24th Fluid Dynamics Conference, 6–9. Orlando, FL, USA. [CrossRef]

Menter, F. R., Kuntz, M., & Langtry, R. (2003). Ten Years of Industrial Experience with the SST Turbulence Model. In K. Hanjali´c, Y. Nagano, & M. Tummers (Eds.), *Turbulence, Heat and Mass Transfer, 4*, 625–632.

Santos, A. L. G., Fragassa, C., Santos, A. L. G., Vieira, R. S., Rocha, L. A. O., Conde, J. M. P., Isoldi, L. A., & dos Santos, E. D. (2022). Development of a computational model for investigation of an oscillating water column device with a savonius turbine. *Journal of Marine Science and Engineering, 10*(1), Article 79. [CrossRef]

Santos, A. L. G. (2023). *Modelagem numérica e método design construtal para avaliação geométrica de um dispositivo do tipo coluna de água oscilante considerando a inserção de uma turbina Savonius* (Tese de Doutorado). Universidade Federal do Rio Grande, Rio Grande, Brasil.

Santos, A. L. G., Petry, A. P., Isoldi, L. A., Dias, G. C., Souza, J. A., & dos Santos, E. D. (2023). Development of a computational model for the simulation of an oscillating water column wave energy converter considering a savonius turbine. *Defect and Diffusion Forum, 427*, 95–106. [CrossRef]

Seibt, F., De, Camargo, Dos, Santos, Das, Neves, Rocha, L. A. O., Isoldi, L., & Fragassa, C. (2019). Numerical evaluation on the efficiency of the submerged horizontal plate type wave energy converter. *FME Transactions, 47*(3), 543–551. [CrossRef]

Temiz, I., Ekweoba, C., Thomas, S., Kramer, M., & Savin, A. (2021). Wave absorber ballast optimization based on the analytical model for a pitching wave energy converter. *Ocean Engineering, 240*, Article 109906. [CrossRef]

Versteeg, H. K., & Malalasekera, W. (2007). *An Introduction to Computational Fluid Dynamics: The Finite Volume Method* (2nd ed.). Pearson Education.

Wilcox, D. C. (2006). *Turbulence Modeling for CFD* (3rd ed.). DWC Industries.